ANNALS OF GEOPHYSICS, VOL. 46, N. 6, December 2003

Ground tilt monitoring at Phlegraean Fields (Italy): a methodological approach

Ciro Ricco, Ida Aquino and Carlo Del Gaudio
Istituto Nazionale di Geofisica e Vulcanologia – Osservatorio Vesuviano, Napoli, Italy

Abstract
Among geodetic methods used for monitoring ground deformation in volcanic areas, tiltmetry represents the most rapid technique and therefore it is used by almost all the volcanological observatories in the world. The deformation of volcanic building is not only the result of endogenous causes (*i.e.* dykes injection or magma rising), but also non-tectonic environmental factors. Such troubles cannot be removed completely but they can be reduce. This article outlines the main source of errors affecting the signals recorded by Phlegraean tilt, network, such as the dependence of the tilt response on temperature and to the thermoelastic effect on ground deformation. The analytical procedure used to evaluate about such errors and their reduction is explained. An application to data acquired from the tilt network during two distinct phases of ground uplift and subsidence of the Phlegraean Fields is reported.

Key words *tilt data – thermoelastic deformation – thermal correction*

1. Introduction

Tilt monitoring is a technique for the identification of some precursors of volcanic eruptions, but it is also a useful tool for the study of the behaviour of volcanoes during post-eruptive phases. Ground tilt measurements are very important because during an inflation episode the flanks of volcanoes deform themselves reaching variations of inclination in the order of about ten microradians.

Such variations happen an almost constant way, but positive gradients of inclination followed by an inversion of the ground tilt recorded during the co-eruptive deflations are not rare (Bonaccorso and Gambino, 1997).

Mailing address: Dr. Ida Aquino, Istituto Nazionale di Geofisica e Vulcanologia – Osservatorio Vesuviano, Via Diocleziano 328, 80124 Napoli, Italy; e-mail: aquino@ov.ingv.it

In order to obtain accurate data, it is necessary to use sensors with resolution suitable to the magnitude of the expected deformation, trying to install them (if possible) symmetrically in relation to the crater, to notice anomalies in the azimuthal deformation, or to different heights to estimate the depth of the source (often dykes), remembering that the maximum slope of the flanks is located at a distance half the depth of the same source (Scandone and Giacomelli, 1998).

In addition to the Phlegraean Fields, Vesuvius, Etna and Aeolian Islands, tilt arrays currently operate in almost all the volcanoes of the world such as (to mention only some of them) Kilauea (Hawaii), Krafla (Iceland), Piton de la Fournaise (Indian Ocean), Galeras and Nevado del Ruiz (Colombia), Tacanà e Fuego (Mexico-Guatemala), Mayon and Taal (Filippines), Merapi and Soputan (Indonesia), Unzen (Japan).

The Phlegraean Fields are a restless caldera located on a NE-SW-trending structure in the graben of the Campanian Plain (fig. 1), formed as a result of the Campanian Ignimbrite eruption, 37 kyr BP, and the Neapolitan Yellow Tuff eruption, 12 kyr BP (Rosi *et al.*, 1995; Orsi *et al.*, 1999). The inter-

Fig. 1. Location of the volcanic area.

est in this area is due to its intense geodynamic and geo-thermal activity, with strong ground uplifts and subsidence episodes (bradyseismic phases), earthquake swarms, and fumarolic emissions. The last eruption dates back to 1538, but major uplifts occurred in 1969-1972 and 1982-1984 when the ground displacements reached a maximum value of 174 cm and 179 cm respectively; these movements refer to the benchmarks (belonging to a Phlegraean levelling line) located in the town of Pozzuoli (fig. 2). The deformation recorded is characterized by an almost bell-shaped form and covers an almost circular area with a radius of 6 km centered in the town of Pozzuoli (Orsi *et al.*, 1999).

The subsidence phase, starting at the end of 1995 and interrupted by three small uplifts (fig. 2), is continuously monitored by the tilt network of the Osservatorio Vesuviano (OV).

2. Historical data

The first clinometric measurements carried out in the Italian volcanic areas con-

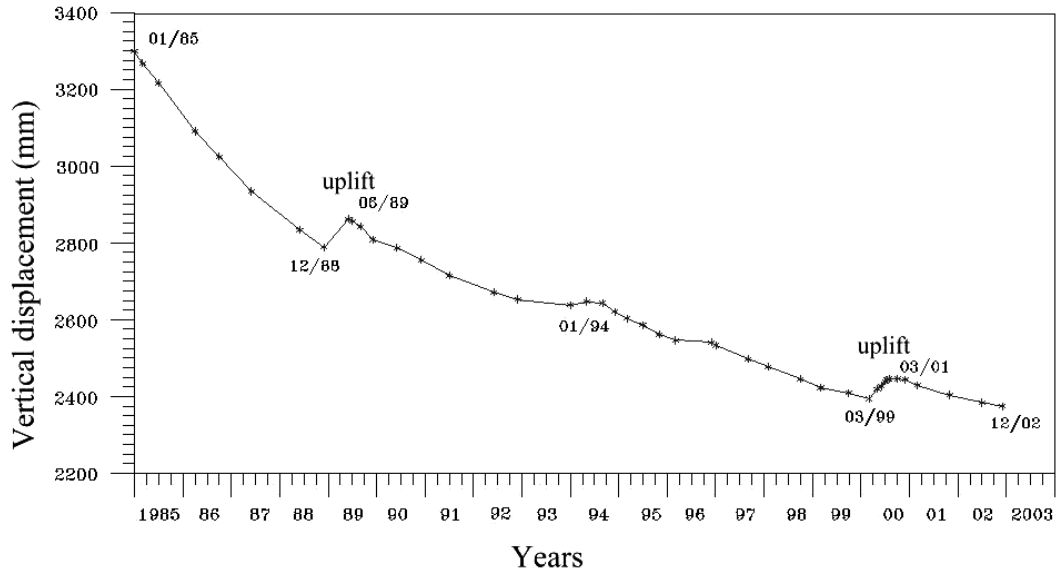

Fig. 2. Vertical displacement of benchmark n. 25 (located in the town of Pozzuoli) over the period 1985-2002
.

cerned Mount Vesuvius and date back to 1935 (Imbò, 1939). The spirit levels placed by Imbò in 1935 on the seismic pillar of the OV historical building (by recording on smoked paper) and oriented N70W-S70E and N20E-S70W measured the apparent deviation of the vertical from October 1935 to January 1939. In 1939, Imbò observed five eruptive intervals (Strombolian activity on the crater bottom) characterized by a fracturing of the intracrateric cone and by lava flows. He noticed an inverse parallelism between the direction of lava flows and the deviation of the vertical and evidenced a direct correlation between the SSW apparent tilt of the volcano and a lowering of the eruptive column, and NNE tilt and the uplifting of the column (Imbò, 1939).

In 1968, two Verbaandert-Melchior horizontal pendulums were installed in the Earth Physics Institute of Naples University (Lo Bascio and Quagliariello, 1968). These were used to compare the clinometric data obtained by other stations located at the base of the Vesuvius cone (Imbò, 1959).

In April 1970, the Institute of Geodesy and Geophysics of the University of Trieste set up a network of four clinometric stations (equipped with two optical tilt sensors with recording on paper, oriented NS and EW) to study the ground deformation caused by the 1970-1972 Phlegraean Fields bradyseismic crisis (Manzoni, 1972) (fig. 2).

3. Tilt network OV – Institute de Physique du Globe (IPG)

In 1987, a tiltmetric network was set up at the Phlegraean Fields (fig. 3) in cooperation with the IPG, which provided the instruments. Each station was equipped with two tiltmeters sensitive along two orthogonal directions, using Zöllner bifilar suspension model, made by P.A. Blum at Paris IPG (fig. 4a,b) (Aste *et al.*, 1986; Briole, 1987). The first station of this type, called DMB, was installed at the end of 1985 in Pozzuoli, and located in a gallery aligned NS, at about 15 m below the surface (figs. 3 and 5). The second station (BAI) was set up in April 1980 in a cistern of Baia Castle; later another

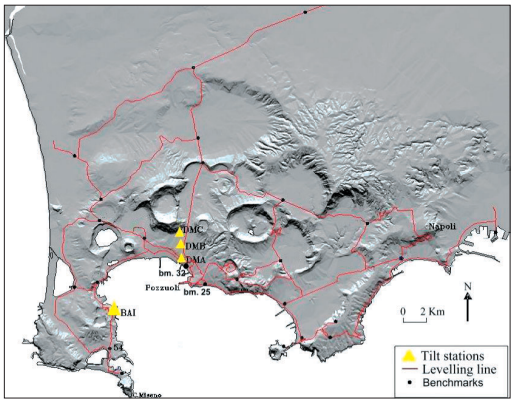

Fig. 3. Levelling line and tilt stations belonging to OV Phlegraean surveillance array.

two stations were set up in October 1987 in Pozzuoli (DMA and DMC) (fig. 3).

The analog signals were digitized through an A/D converter on a Canon X-07 computer (fig. 4b).

The stations DMB and BAI initially worked with an 8 bit acquisition program allowing data accumulation in the RAM memory with a sampling rate between 1 and 60 cph. The data were recorded in both graphic and numerical form.

Later, a 12 bit acquisition program was used to control the operation of the whole system, *i.e.* switch the bulb on and off, reception analogical signal, digital conversion and data accumulation. The fundamental difference from the first 8 bit acquisition program was that the latter program turned on the tilt station only in the time period of sampling and therefore the electric absorption of the installation was reduced.

Data in memory were periodically transferred onto a cartridge directly in the field, through the same program and later were sent to a PC through an RS232 Serial interface (Luongo *et al.*, 1988).

4. Automatic tiltmeter network

Between 1991 and 1992, the stations equipped with the pendulums were replaced by stations with electronic sensors, easier to

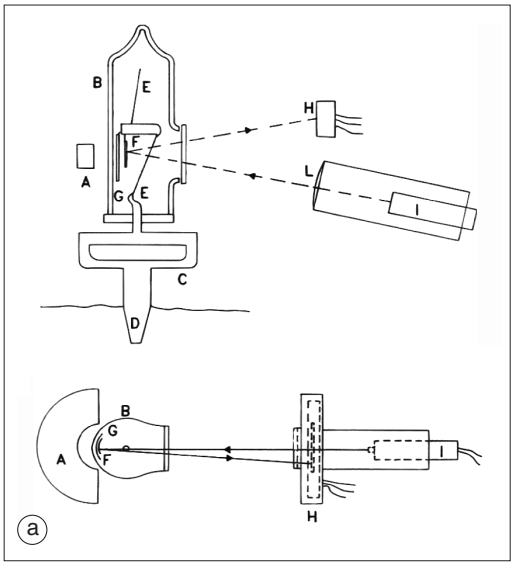

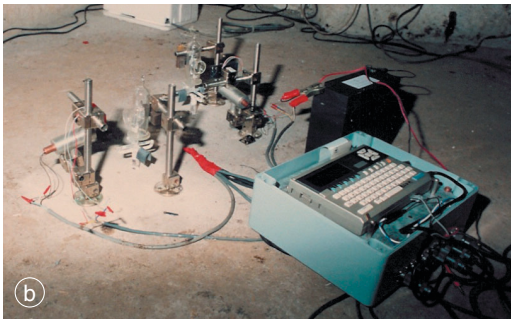

Fig. 4a,b. a) Section, view from the top of Blum's optic clinometer. All the pendulum mobile parts E, which are made of silica (with a coefficient of thermal dilatation $\beta = 0.54$ ppm/°C), are contained in a pyrex bell B under vacuum. The pendular part is formed by a concave mirror F joined to the silver plate G, which dampens the oscillations through Foucault currents excited by a magnet near A. The pendulum is tightly anchored to the soil through a silica cone D fixed in the hole on the base C. The pendulum rotation is linearly transduced into a variation in voltage through the coupling lamp I, mirror, photocell H. The main limit of this apparatus in highly dynamic areas is due to the regular check of the pendulum oscillation period since it is a function of the pendulum tilt (Aste *et al*., 1986, modified). b) Tiltmetric station OV-IPG installed at Pozzuoli (DMB) and working from the end of 1985 to 1992. The picture shows the pair of transducers and the acquisition unit.

handle and to install. These sensors were biaxial, bubble-type, short baselength platform tiltmeters, manufactured by Applied Geomechanics (AGI)-Mod. 702 A (AGI, 1997). These instruments are made of steel and contain two transducers (one for each axis) formed by a glass case closed at the ends by three electrodes and containing an electrolytic liquid. The case is enclosed in a bridged electric circuit; the inclination of the ground produces a voltage proportional to the amount of resistance imbalance. The tiltmeter is also equipped with a temperature sensor. The signals recorded by each sensor are A/D converted and recorded automatically at a sampling rate between 6 and 60 cph. The station also acquires the supply voltage before the telematic connection with the Monitoring Center at OV in Naples. In 1993, another station (OVO) of this type was lodged on a pillar of armed cement inside a gallery at 25 m depth from the surface, near the OV historical building at Ercolano (Mount Vesuvius). OVO is 2.5 km WNW from the crater of the volcano. In 1996, another two stations were set up at Trecase, in the Forestry Barrack (TRC) and at Torre del Greco (CMD). TRC and CMD are located 2.5 km SSE and to 5 km SSW from the crater, respectively.

Today, the whole network is formed by the Vesuvian (fig. 6) and Phlegrean arrays (fig. 3).

5. Tiltmeter applications and instrumental characteristics

The long-period tilt monitoring of a volcanic region may help to derive the geometry and the speed of the deformation of the studied area. Obviously, it is important to compare the acquired tilt data with those obtained from other techniques.

The possibility to use electronic tiltmeters is closely connected to the mechanic and electronic features of the sensor (resolution, accuracy/repeatability, range of measure and drift), and is influenced by the dependence on environmental factors (coupling to the surface, temperature, atmospheric pressure, rainfall, oscillation of the water table, freeze-thaw cy-

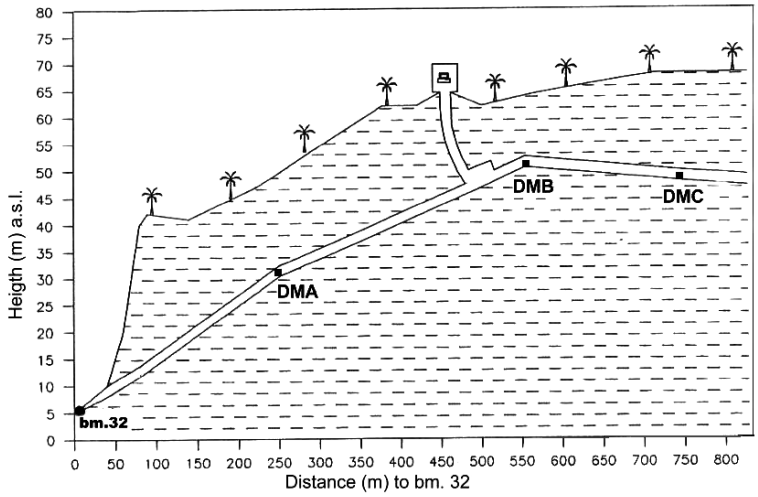

Fig. 5. Topographical section of subsurface gallery in Pozzuoli and the DMA, DMB, DMC position.

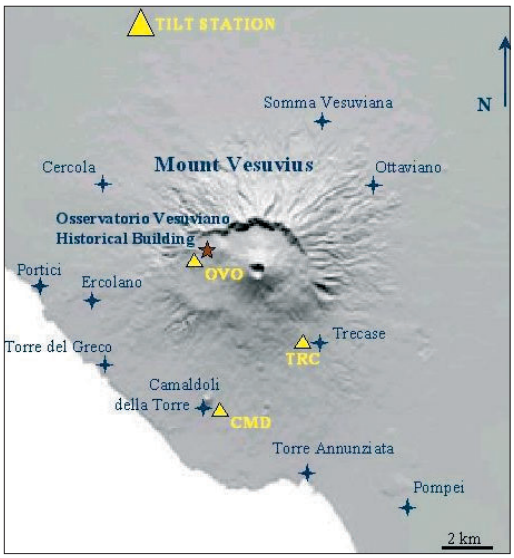

Fig. 6. OV Vesuvian tiltmeter array.

cles) (Dzurisin, 1992; Braitenberg *et al.*, 2001). The surface sensors AGI have an angular range of ± 800 microradians (μrad) in High Gain (HG) and of ± 8000 μrad in Low Gain (LG), a resolution of 0.1 μrad, a sensitivity of 10 mV/μrad, a repeatability of 1 μrad, a maximum non linearity of 1% (HG) and 3% (LG).

The *resolution* represents the minimum angular variation measured by the device (μrad) while the *sensitivity* is the ratio between the instrumental to the angular response (mV/μrad). The sensitivity setting in high gain enhances the quality of the information on tilt variations even if the available angular range is reduced. However, in our case, this is not a limitation since the monitored volcanic areas are not affected by deformations large enough to require the larger angular range.

Repeatability shows the deviation among several readings referred to the same angular magnitude. Repeatability can be considered the absolute error of the measurement itself. *Maximum non linearity* is the ratio between the maximum residual $\left(y_i^{\max} - \hat{y}_i\right)$ recorded during the calibration of the sensor (that is the recording on a calibration plate at a steady temperature T_{cal} of the output voltages of the sensor subject to a range of known tilts) to the whole calibration angular range.

The angular coefficient of the calibration line gives the *scale factor* SF_{cal} (expressed in μrad/mV; AGI, 1998).

6. Dependence of the device response on temperature and compensation

The installation of tiltmeters to derive the ground deformation pattern must be done with great care, as bubble-tiltmeters are very sensitive to temperature changes. The transfer of heat from the air to the soil and the solar radiation heating the ground, during the day, both on the surface and close by.

These temperature variations cause a first order effect on the surface tiltmeters, mainly if the medium is heterogeneous. This effect is proportional to the thermal dilatation (β) of the screws made of invar mounted at the base of the sensor; these screws have to be therefore of the same length.

Instead, borehole tiltmeters have a radial symmetry and therefore are affected by volumetric strain changes. These tiltmeters are installed at depth, where thermal oscillations are minimum. Even the electrolytic transducer is subject to thermal fluctuations since the liquid is subjected to contraction and expansion with the consequent change of SF_{cal} and with zero shift (AGI, 1995).

If we do not take into account these effects due to the difference between the environmental temperature (Te) and the calibration temperature (T_{cal}), the measured tilt angle will be different from the real one. The thermal compensation is calculated through the two coefficients of correction K_s and K_z experimentally measured in the laboratory

$$K_s = \frac{(SF - SF_{\text{cal}})}{SF_{\text{cal}}} \cdot \frac{1}{(Te - T_{\text{cal}})}$$

(*i.e.* the change in slope of the calibration line per unit Te change)

$$K_z = \frac{(SF_{\text{cal}} \cdot V_T) - \text{Tilt}_{\text{app}}}{(Te - T_{\text{cal}})}$$

(*i.e.* the zero shift per unit Te change) where T_{cal} is the calibration temperature, SF_{cal} is the scale factor at T_{cal}; Te, the environmental temperature; SF, the scale factor at Te; V_T, the output voltage when the sensor is perfectly horizontal; Tilt_{app}, the apparent tilt angle.

The coefficient K_s and K_z of the surface sensors AGI (in high gain) are respectively equal to 0.04%/°C and to 1.5 μrad/°C.

The reduction of the error is determined by the following equation:

$$\text{Tilt} = SF_{\text{cal}}\left[1 + K_s(Te - T_{\text{cal}})\right] \cdot \cdot V - K_z(Te - T_{\text{cal}}) \qquad (6.1)$$

where V is the output voltage and Tilt is the compensated tilt.

7. Thermal damping in the soil

The compensation of the tilt signal to Te does not correct the thermoelastic strain of the ground. This effect is present in the signals recorded by surface tiltmeters and may hide the ground tilt linked to volcanic activity, thereby modifying the spectral content of the signals. In order to dampen the thermal excursions, the surface sensors are generally installed in caves. The best installation is achieved positioning the borehole tiltmeters in holes deeper than 10 m (Jentzsch *et al.*, 1993; Weise *et al.*, 1999).

The phenomenon of thermal damping concerns the modality of propagation of the thermal wave in the ground, which, on the surface, follows the oscillation of the solar radiation according to two main periods, a daily and a yearly period.

The surface temperature oscillation can be represented as a sinusoidal and stationary wave

$$Te = A\cos(\omega t) \qquad (7.1)$$

where $\omega = 2\pi / T$ is the angular frequency; T, the period of the wave; t, the time and A, the amplitude of the wave.

Hypothesizing the subsurface as a homogeneous half space in which the isotherms are parallel, the heat conduction takes place according to Fourier's equation (Persico, 1962)

$$\frac{\partial^2 Te}{\partial z^2} = \frac{1}{D} \cdot \frac{\partial Te}{\partial t} \qquad (7.2)$$

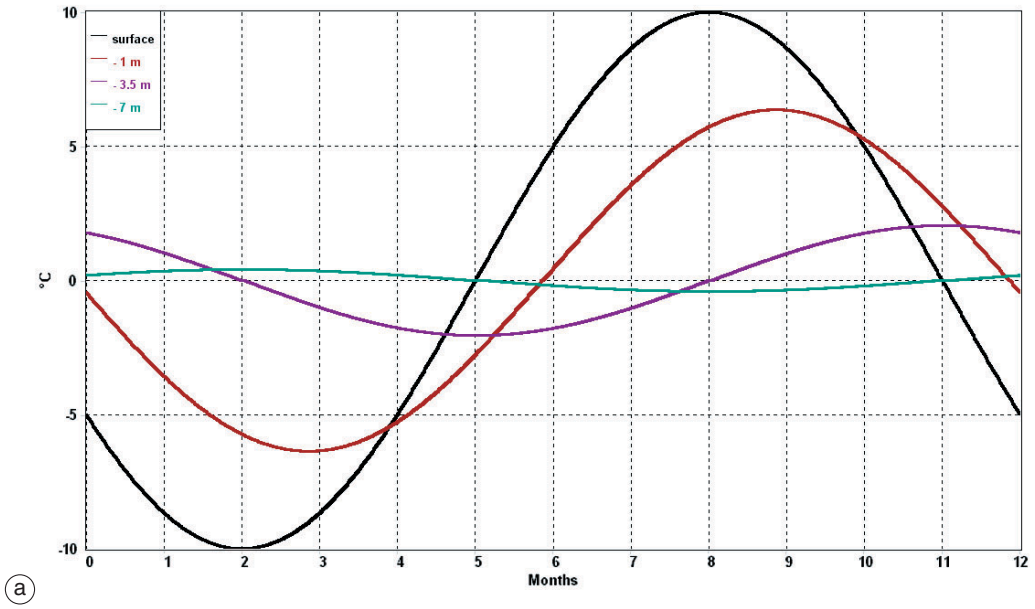

a

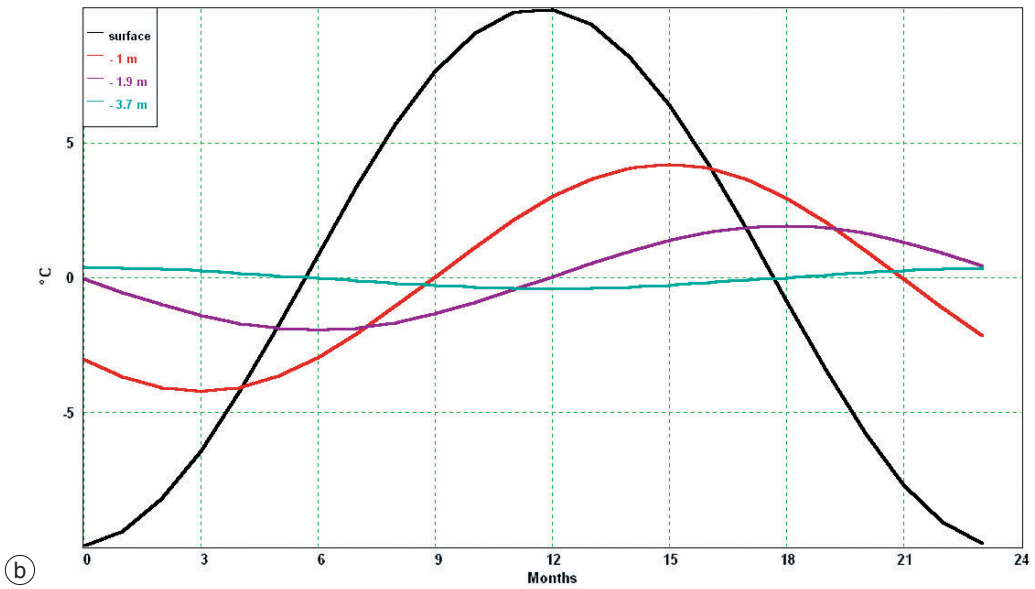

b

Fig. 7a,b. Theoretical thermic attenuation of an annual wave with parameters: a) $D \cong 0.0018$ m^2/h, $\alpha = 0.451$ m^{-1}, $\lambda = 13.935$ m, $\lambda/T \cong 0.038$ m/d (the phase opposition occurs at a depth of 7 m); b) $D \cong 0.0018$ m^2/h, $\alpha = 8.614$ m^{-1}, $\lambda = 0.729$ m, $\lambda/T \cong 0.03$ m/h (the phase opposition occurs at a depth of 0.37 m).

where $D = K / c\rho$ is the thermal diffusivity ($\cong 0.0018$ m^2/h in the soil); K, the thermal conductivity; c, the thermal capacity; ρ, the density; and z, the depth.

Replacing eq. (7.1) with eq. (7.2) and successively integrating Fourier's equation, the attenuation and delay of the thermal wave in function of the depth and of the characteristics of the medium crossed is determined by

$$Te_{(z)} = Ae^{-\alpha z}\cos(\omega t - \alpha z)$$

where $\alpha = \sqrt{\omega/2D} = \sqrt{\pi/Dt}$ is the attenuation factor.

The rate of thermal wave propagation is

$$\frac{\lambda}{T} = 2 \cdot \sqrt{\frac{\pi D}{T}}.$$

The thermal wave is therefore a sinusoidal function of time and decreases exponentially with depth according to α. The reduction of the amplitude will be higher for a shorter period of the wave or for a longer wave path. Moreover, the thermic wave is also subjected to a time delay, which causes a phase shift in comparison to the incident wave. The phase shift of 180° occurs at the depth

$$z = \frac{\pi}{\alpha}.$$

In a ground with thermal diffusivity of 0.0018 m^2/h, a yearly thermic excursion of 20 °C would be reduced to 0.2 °C at a depth of 10 m. The thermic wave would have a speed of propagation of 0.038 m/d (fig. 7a); the same diurnal excursion would be reduced to 0.002 °C at a depth of 1 m. The wave would have a speed of propagation of 0.03 m/h (fig. 7b).

8. Thermoelastic deformation

The heat propagation causes a deformation within rocks. According to the bidimensional model proposed by Berger (1975), in an elastic infinite homogeneous half space, a traveling temperature wave on surface is represented by

$$Te_{(z)} = Ae^{-\gamma z}e^{i(\omega t + \kappa x)}$$

where $\gamma = \kappa\sqrt{1 + i\omega/D\kappa^2}$ is the attenuation factor, $\kappa = 2\pi/\lambda$, the horizontal wave number and i, the imaginary unit; causes the dilatation of the medium

$$\varepsilon_{ij} = \beta Te\delta_{ij}$$

where β is the linear thermal dilatation coefficient; δ_{ij} is the Kronecker Delta

$$\Delta = \left|\begin{matrix} 1 & i = j \\ 0 & i \neq j \end{matrix}\right.$$

and i, j are the indexes referred to the coordinated axis.

The strain ε_{ij} is the second term of the following equation related to the plane XZ and describes the infinitesimal displacement of the around of a point in a continuous medium

$$u_x + du_x = u_x + \frac{1}{2}\left(\frac{\delta u_x}{\delta z} + \frac{\delta u_z}{\delta x}\right)dz + \frac{1}{2}\cdot \cdot\left(\frac{\delta u_z}{\delta x} - \frac{\delta u_x}{\delta z}\right)dz = u_x + \varepsilon_{xz}\,dz + \omega_{xz}\,dz. \tag{8.1}$$

The partial derivatives in eq. (8.1) are the elements of the strain tensor E and of the rotation tensor Ω (Zadro and Braitenberg, 1999).

Berger's (1975) solution allows to calculate the thermoelastic Tilt in the following way:

$$\text{Tilt}_{(z)} = \frac{\delta u_z}{\delta x} = i\left(\frac{1+\sigma}{1-\sigma}\right)\left(\frac{\kappa}{\gamma}\right)\cdot\{[(1-2\sigma) - \kappa z]\cdot \cdot e^{-\kappa z} + e^{\gamma z}\}\cdot\beta A e^{i(\omega t + \kappa x)}$$

where σ is the Poisson's ratio.

It can be noticed how the Tilt is mainly formed by two terms exponentially decreasing with depth, $e^{-\kappa z}$, which is related to the existence of superficial tractions caused by thermal stresses in the layer (whose depth is $2\pi/\gamma$), and $e^{-\gamma z}$, which is due to a body force resulting from the gradient of temperature at depth.

Since, in practice, the most important variations of temperature occur at period of the order of the hours, assuming $\lambda = 10^3$ m or longer and $D = 10^{-3}$ m^2/h, $\gamma \cong (1 + i)\sqrt{\omega/2D}$.

A more complete solution, which takes into account the surface topography (valid only for

slopes that are uniform over a long distance), was found by Harrison and Herbst (1977)

$$\mathrm{Tilt}_{(z)} = 0.5 \cdot \left(\frac{1+\sigma}{1-\sigma}\right) \beta A e^{-\alpha z} \cdot \cdot \cos(\omega t - \alpha z) \cdot \sin(2\varphi)$$

where φ is the surface slope in degrees.

This model, however, does not take into account the Berger (1975) traction term $e^{-\kappa z}$ and therefore underestimates the theoretical Tilt.

9. Other sources of error in the tiltmetric signal

Other sources of perturbations on the tiltmetric signal are water table variations (Kümpel, 1983) and rainfalls (Wolfe *et al.,*1981; Kümpel, 1986; Braitenberg, 1999), which tend to modify hydrostatic pressures acting in permeable rocks and therefore cause deformations, but also the height variations of the sea-level, when the stations are near the sea. Also, the strong atmospheric perturbations can disturb on the signal but their non-periodic effects are generally superimposed on those produced by the periodic tides. Other non-tectonic signals recorded by tiltmeters are the atmospheric pressure loading (Dal Moro and Zadro, 1998), ocean loading (Davis *et al.*, 1987) and earth tides (Sleeman *et al.*, 2000). All these causes can create a systematic component in the measurement of the ground inclination that masks the deformation induced by the volcanic activity.

Another source of systematic error is the site effect, which includes lateral inhomogeneities in rock/soil properties and the cavity effect (Harrison, 1976; Zadro and Braitenberg, 1999).

For the surface tiltmeters, it is necessary to realize a stable coupling to the rock. The ground coupling is not quantifiable; testing consists in the periodic verification of setting that is effected by slightly compressing the ground in proximity of the sensor alternatively along the sensitivity directions of bubbles and verifying the recorded tilt values.

After this test, the sensor will acquire its new position of balance, which must coincide with the one previously taken.

10. Data acquisition and processing

For each station of the OV tilt network, four series of signals acquired in real time are available; the first two are the signal acquired by NS and EW components, the third one concerns air temperature at the soil level and the last is the supply voltage. The acquisition frequency is currently of 6 cph at BAI, CMD and OVO, of 2 cph at DMA, DMB and DMC, and of 360 cph at TRC (table I).

The signal is analized using equal criteria for each station, but the software used differs according to the age of the station itself as well as to the format of the raw data and to the noise present in the monitored site. The final format of all the data acquired is defined by standard criteria. The most recent station dates back to 1996 and the oldest one to 1991.

The following phase of elaboration uses graphic-analytical procedures implemented through the software DADISP by DSP Development Corporation (Dadisp, 1996).

The signal is cleaned by detecting possible offsets and spikes connected to differences in supply voltage of the stations; spikes are immediately removed through polynomial detrending and anomalous values residuation, while the offsets and the possible interruption in acquiring data compel us to operate on the signal replacing gaps by null values or constant values. The thermic compensation of the tilt recorded by the two components and the conversion from mV to μrad are performed with eq. (6.1).

Afterwards, the EW and NS components are combined to a vectorial plot of the tilt variation over time.

Every point recorded by the plot is defined by a pair of values (Tilt^t_{EW}, Tilt^t_{NS}) referred to time t. Each variation ($\mathrm{Tilt}^{t+n} - \mathrm{Tilt}^t$) represents the ground tilt recorded over the nth time period characterized by both the modulus and the direction.

The adjustment and the orientation of the biaxial sensors is pursued in such a way that positive and negative values indicate NE sinking and uplift respectively. The tilt variations are such that

$$\text{northward down if } \mathrm{Tilt}^{t+n}_{NS} > \mathrm{Tilt}^t_{NS}$$
$$\text{eastward down if } \mathrm{Tilt}^{t+n}_{EW} > \mathrm{Tilt}^t_{EW} .$$

Table I. OV tilt network: description and technical features.

Station	Sensor	Number	Latitude	Longitude	Depht a.s.l.(m)	Depht (m)	Place	Description	Installation date
DMA	AGI 702	1219	40°49′57″	14°06′47″	30	−18	Pozzuoli	Gallery	March 1991
DMB	AGI 702	1158	40°50′06″	14°06′46″	50	−13.5	Pozzuoli	Gallery	March 1991
DMC	AGI 702	419	40°50′12″	14°06′46″	48	−20.5	Pozzuoli	Gallery	March 1991
BAI	AGI 702	1593	40°48′29″	14°04′26″	20	0	Baia	Cistern of Castle	June 1992
OVO	AGI 702	1592	40°49′36″	14°23′52″	608	−25	Ercolano	Historical building OV	February 1993
TRC	AGI 702	2539	40°47′47″	14°25′22″	150	0	Trecase	Forestry barrack	March 1996
CMD	AGI 702	2537	40°46′40″	14°24′23″	120	−2	Torre del Greco	Surface well	June 1996

Station	Sampling rate (cph)	A/D conv. (bit)	SF_{CAL} (μrad/mV) high gain	Sensitivity (mV/μrad)	T_{CAL} (°C)	T_{SF} (°C/mV)	K_S (%/°C)	K_Z (μrad/°C)
DMA	2	12	0.09960 $X_{(NS)}$ 0.10018 $Y_{(EW)}$	10.0-09.9	21	.1	0.05	1.5
DMB	2	12	0.09936 $X_{(NS)}$ 0.10005 $Y_{(EW)}$	10.1-10.0	27	.1	0.05	1.5
DMC	2	12	0.10000 $X_{(NS)}$ 0.09615 $Y_{(EW)}$	10.0-10.4	22	.1	0.05	1.5
BAI	6	12	0.09964 $X_{(NS)}$ 0.10030 $Y_{(EW)}$	10.0-10.0	21	.1	0.05	1.5
OVO	6	12	0.09965 $X_{(NS)}$ 0.10000 $Y_{(EW)}$	10.0-10.0	20	.1	0.05	1.5
TRC	360	12	0.10000 $X_{(NS)}$ 0.10010 $Y_{(EW)}$	10.0-10.0	17.3	.1	0.05	1.5
CMD	6	12	0.09964 $X_{(NS)}$ 0.09947 $Y_{(EW)}$	10.0-10.1	16	.1	0.05	1.5

Tilt direction is calculated clockwise moving from N over time, whereas the percentage of counts of each recorded azimuth is shown by a histogram.

11. Spectral content of the acquired signals

Up to now, we considered the most important steps by which we work out the tilt temporal tendency in a certain station. However, the above mentioned ground tilt still present part of deformation due to the thermoelastic response of the rocks that, as we have already seen, may be disregarded only if we use sensors placed in a very deep well. Spectrum bands, where thermoelastic effects are more likely to be produced, coincide with the diurnal and annual components.

These bands may be very easily identified, analysing the thermal and ground tilt data in the frequency domain using the Fast Fourier Transform (FFT) algorithm (Oppenheim and Schafer, 1975) into the DADISP environment.

Figure 8a,b compares the spectrum of the tilt signal (NS component) from station BAI to the spectrum of the temperature recorded by the sensor. The interval considered is four years (from 1998 to 2001). The prevailing of 24 h component (Jentzsch *et al.*, 2002) is noticed in both spectra while the tilt signal gives the main semi-diurnal constituents of the tidal spectrum (Melchior, 1978; Ricco *et al.*, 2000).

The removal of the effect caused by thermoelastic soil deformation is a much debated problem, because the action of filtering the spectrum components of solar provenance through the Tilt signal inevitably modifies the signal itself, particularly at periods of the order of months.

This can even interfere, in some way, with the understanding of the pattern of ground deformation in volcanic areas. On the other hand, we have experimentally proved that, as concerns tiltmeter data acquired by OV, frequency filtering is likely to bring more reliable results at least regarding diurnal and se-

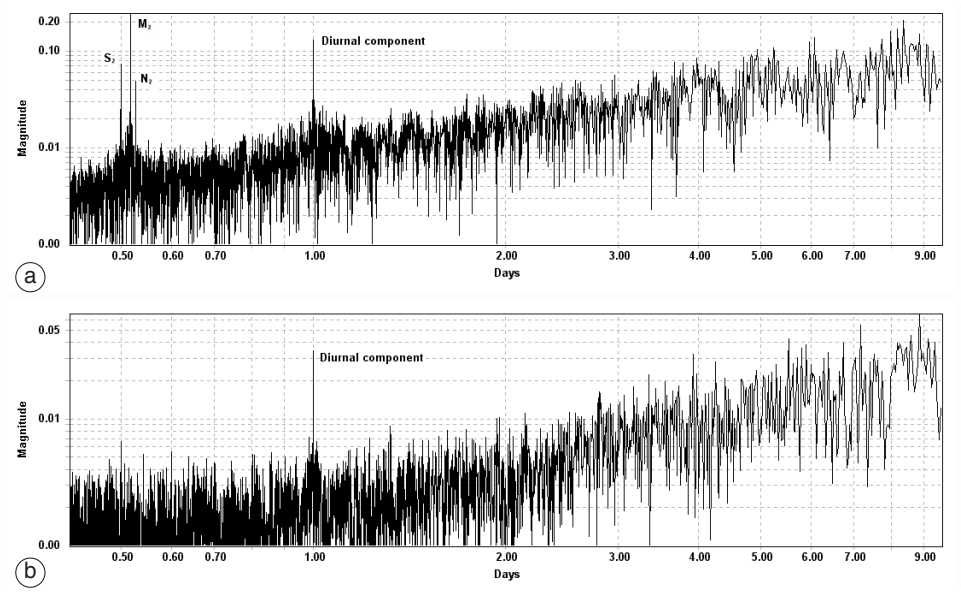

Fig. 8a,b. Spectral analysis of Tilt and *Te* signals recorded by BAI station over the years 1998-2001 (210384 data points with a sampling frequency of 6 cph). Thermal components given by the two signals are to be ascribed to the thermoelastic ground deformation. The semi-diurnal components, not given by the *Te* signal, are related to the influence of sea tide in the Baia Gulf but also to that of earth tide components: a) FFT of Tilt data (μrad) and (b) FFT of the *Te* data (°C).

mi-diurnal components. Otherwise, for longer periods, other analysis techniques must be implemented. The procedure adopted to remove periods lasting more than 8 h is shown in fig. 9a-n for the signals from TRC station.

12. Tilt recording of superficial earthquake waves

The filtering procedure shown in fig. 9a-n concerns the recording made on the 18th April 2002. Some surface waves caused by the earthquake that hit the Lucano Appenines (latitude 40.612, longitude 15.594, depth 4.5 km, local magnitude 4.1) on that date are recorded in the tilt components. Figure 10a,b depicts 20 min of the signal shown in fig. 9a-n. A large number of regional earthquakes of magnitude larger than 4 and a good number of teleseismic events have been recorded by the TRC station and the OVO station, although the latter has a sampling frequency 60 times less than that of TRC.

13. Application of a statistical procedure of thermal correction to a tilt data

We have quantified Tilt dependence on the temperature through a linear model of type $\hat{y} = a_0 + a_1 x$, but this can also be done applying a polynomial model of type $\hat{y} = a_0 + a_1 x + a_2 x^2 + \ldots + a_n x^n$ where n is the polynomial order.

Assuming *Te* as the independent variable, the relation between the recorded thermal data and the average of the ground tilt data can be worked out through a linear least square regression model. Assuming that every Tilt value has a Gaussian distribution, it is possible to obtain, by a dispersion diagram of the pair of values (Te_i, Tilt_i), the

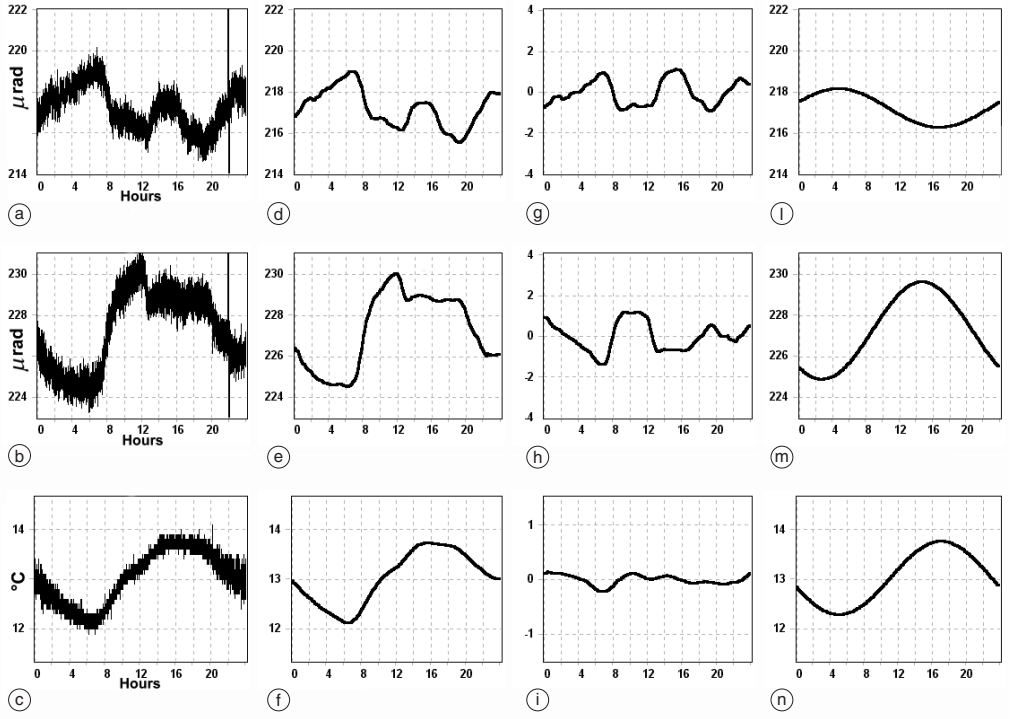
μrad
Hours
°C
a
b
c
d
e
f
g
h
i
l
m
n

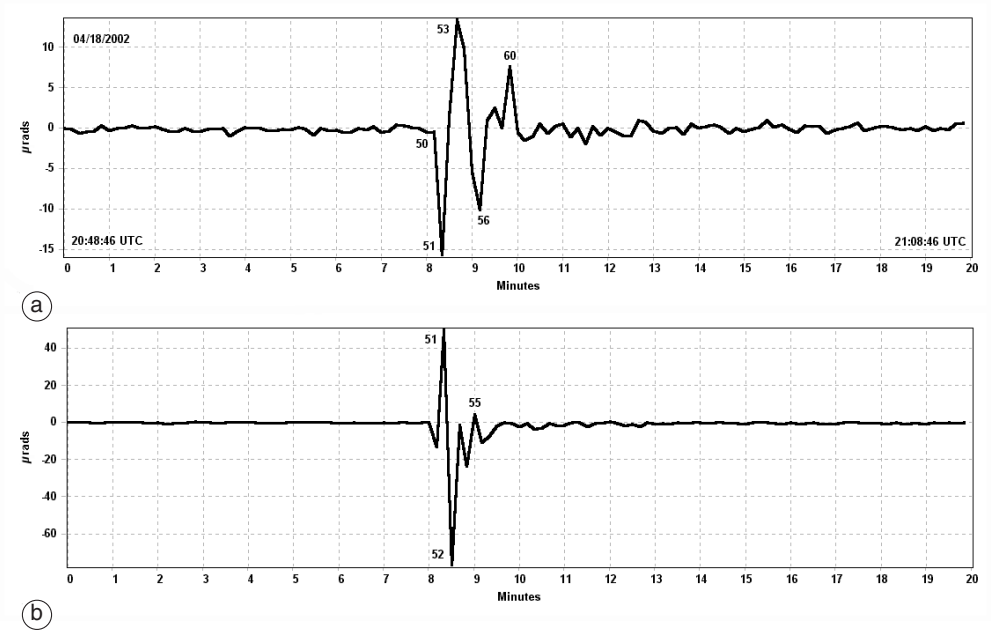
04/18/2002
20:48:46 UTC
21:08:46 UTC
μrads
Minutes
53
60
50
56
51
55
52
a
b

'best' interpolating curve containing the necessary data to minimize the residual sum of squares $y_i - a_0 - a_1 x = y_i - \hat{y}_i$ (Davis, 2002).

From the solution of the so-called *normal equations*, a_0 and a_1 (which define the parameters of the linear model we were looking for) are obtained. In this case, the intercept of the best straight line is a_0 and its slope or regression coefficient is a_1. We have verified that the assumption of the linear dependence Tilt = f (*Te*) can be held as effective only in those intervals in which *Te*, previously filtered at high frequencies, shows an increasing or decreasing trend in time.

The yearly *Te* signal recorded is decomposed in a table with n subseries having *Te* values and whose trend is highly increasing or decreasing, according to a spectral band having frequencies lower than 1 cpd. Then, n matrices with 2 columns are developed, each of them containing couples of ordered values (*Te,* Tilt), which allowed us to calculate the n best straight lines.

Afterwards, the difference between the n subseries of the original tilt data and n best straight line will be calculated and the whole table so unravelled creating a single vector; obviously, this is done after having deducted the relevant offsets. The new signal so computed is very much less correlated to temperature than the original one. Moreover, for each subseries, the following statistical indicators are calculated:

i) The Bravais-Pearson linear correlation coefficient R (equal to the ratio between the covariance of two variables to the product of their standard deviations), which indicates the degree of interrelation between variables $Te = x$ and $\text{Tilt}_{NS} = y$.

ii) The regression coefficient a_1 (already defined).

iii) The standard error of the estimate σ (equal to the square root of the ratio between the residual sum of squares of y to $n - 2$).

These indicators immediately verify the goodness of fit.

In this procedure, that we call *thermal decorrelation*, a linear model is assumed to simplify the calculus, but linearized or more complex models, may be also assumed.

14. Monitoring of ground movement

At Phlegraean Fields, tilt monitoring allowed us to detect from 1988 a deflation phase confirmed by levelling data. The maximum vertical displacement observed between 1988 and 2001 was – 405 mm in Pozzuoli (fig. 2). The main uplift which interrupted the ground subsidence occurred during the first six months of 1989 (74 mm uplift at Pozzuoli) and induced a 90° tilt rotation clockwise at DMB station (Ricco *et al.*, 1991, 1994) (fig. 11). Unfortunately, the other stations did not record remarkable variations of ground inclination.

The tilt network recorded the following ground lowering and, in the year 2000, a new

Fig. 9a-n. Example of how components lasting more than 8 h and concerning the signals recorded by TRC station on the 18th April 2002 are filtered. In (a), (b) and (c) the two tiltmeter signals and the termic one, acquired every 10 s, are shown respectively, while in (d), (e) and (f), the signals undergo a 1 h moving average procedure, which allows us to reduce noise. In (l), (m) and (n) the Inverse Fast Fourier Transform (IFFT) of the smoothed signals are computed, highlighting only harmonic content having a period of time lasting more than 8 h. In (g), (h) and (i) harmonic having a period of time lasting less than 8 h are shown: a) NS signal, d) smoothed data, g) high pass data, l) low pass data; b) EW signal, e) smoothed data, h) high pass data, m) low pass data; c) *Te* signal, f) smoothed data, i) high pass data and (n) low pass data.

Fig. 10a,b. Tilt variations induced by an earthquake with epicentral distance of 1.2°. In this figure, 20 min (120 data points) of the NS (a) and EW (b) signals recorded at TRC station are shown. The followings numbers close to the peaks point out the main variations of the signals: 50th acquisition at 20:56:56 UTC; 51th at 20:57:06 UTC; 52th at 20:57:16 UTC; 53th at 20:57:26 UTC; 55th at 20:57:46 UTC; 56th at 20:57:56 UTC; 60th at 20:58:36 UTC.

trend inversion over the March-August period (confirmed by levelling data showing an uplift of 28 mm centered at Pozzuoli); this is quite clear for both the signals acquired from 1998 to 2001 at DMB (fig. 12a-c). In this figure it is possible to observe that the tilt components show, during the middle months of 2000 and in correspondence with a similar thermal trend, an opposite trend with respect to that of 1998, 1999 and 2001 (Achilli *et al.*, 2001).

In these three years, the ground tilt average occurred in the SE sector, in correspondence with the first 8-9 months of each year (corresponding to the ground *Te* increase) and in the NW sector during the remaining months (corresponding to the ground temperature decrease). Otherwise, in the year 2000, the uplift phase due to the bradyseism affects the tilt vector trend, reversing its direction.

We can note that the annual component on tilt signals decreases during 2000 because the inversion of the tilt direction is verified. In quantitative terms, the linear regression and correlation coefficients between *Te* and Tilt calculated during 2001 (– 4.49 μrad/°C and – 0.92 for NS component, 2.92 μrad/°C and 0.86 for EW component respectively), during 1999 (0.67 μrad/°C and 0.32, 3.59 μrad/°C and 0.79) and during 1998 (– 1.91 μrad/°C and – 0.66, 3.59 μrad/°C and 0.76), appreciably result different from those calculated during 2000 (– 0.63 μrad/°C and – 0.21 for NS component, 0.35 μrad/°C and 0.27 for EW component).

It is plain that the comparison of the signals in the different years is very useful because it reveals the possible anomalies in comparison to a «normal» trend that, in this volcanic area, is represented by the subsidence phase. However, when we have few data, or when the geometry of the deformation is not known or is complex, or when we want to know only the variations of the inclination induced by volcanism, it is necessary somehow to eliminate the thermal effect.

For thermal correction we chose the NS component of the DMB station because it recorded the Phlegraean deformation in the best way. The test concerned the years 2000 and 2001 with the intent to obtain both a sufficiently filtered signal but mainly to verify if the tilt record in the year 2000 succeeded in discriminating the uplift. The

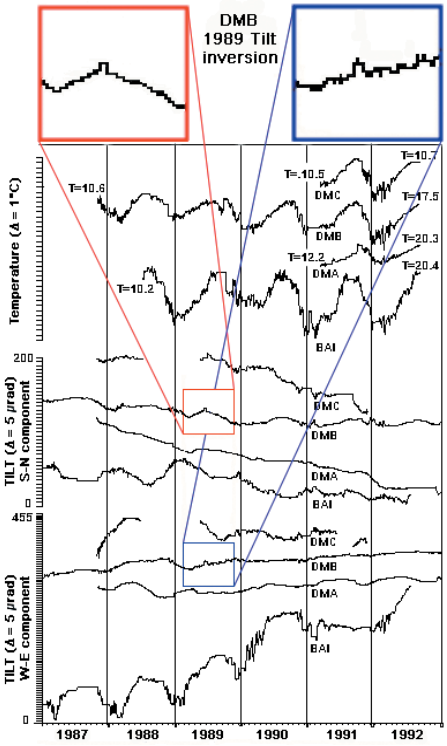

Fig. 11. Ground Tilt and *Te* recorded by the network OV-IPG in the period 1987-1992: every signal includes more than 100.000 data points with sample rate of 1 cph. The zoomed windows concern the uplift phase. Tilt decrease must be interpreted as sinking (southward and westward down) otherwise as uprising.

Te signals were decomposed into 87 subseries, (each of which ended with a peak or valley) and the application of statistical procedure to a NS tilt component produced a corrected signal showing an inclination towards N beginning by the middle of March (fig. 13a-d). The statistical indicators R and σ related to the subseries indicate a good fit (fig. 13a-d).

The same application was performed on *Te* data recorded in 2001; in this case the sequence was decomposed into 124 subseries and the decorrelated NS signal underwent a contraction in comparison to original one but still showed an inclination towards S throughout the year (subsidence) (fig. 14a-c). Also R and σ were

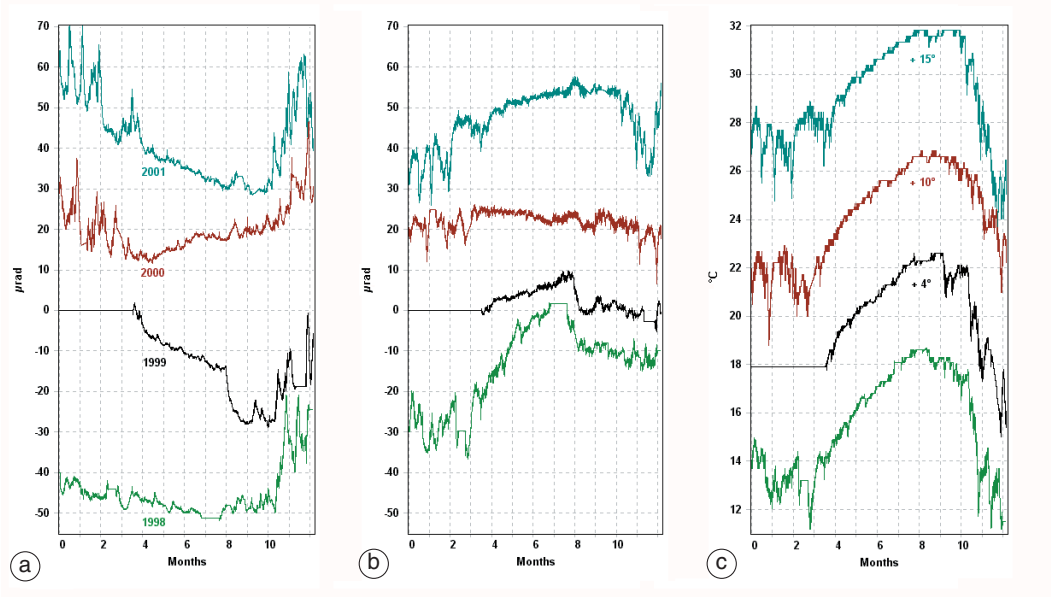

Fig. 12a-c. This figure shows a comparison between Tilt NS (a), EW (b) and *Te* (c) recorded at DMB station over the years 1998, 1999, 2000 and 2001. Note the opposite trend in the NS (a) and EW (b) components recorded in 2000.

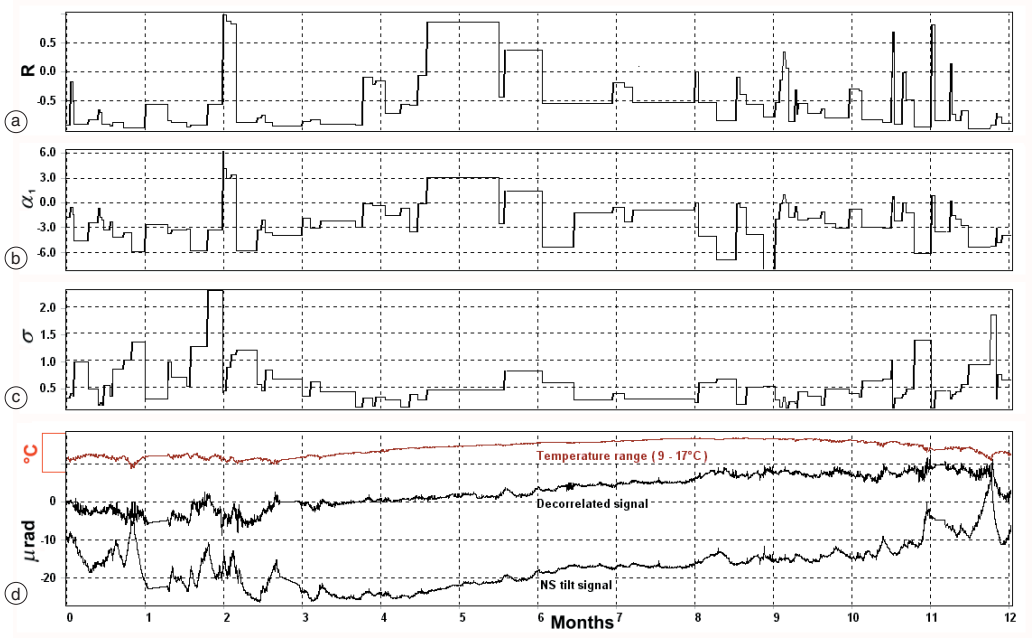

Fig. 13a-d. Application of a statistical procedure of thermal decorrelation to the NS component of the tilt recorded by DMB in 2000 through a linear dependence model. In (a), (b) and (c) the correlation coefficients, the regression coefficients (μrad/°C) and the standard errors of the estimate (μrad/$\sqrt{n-2}$) are displayed, respectively. The corrected signal (d) shows an inclination towards N (ground uplift).

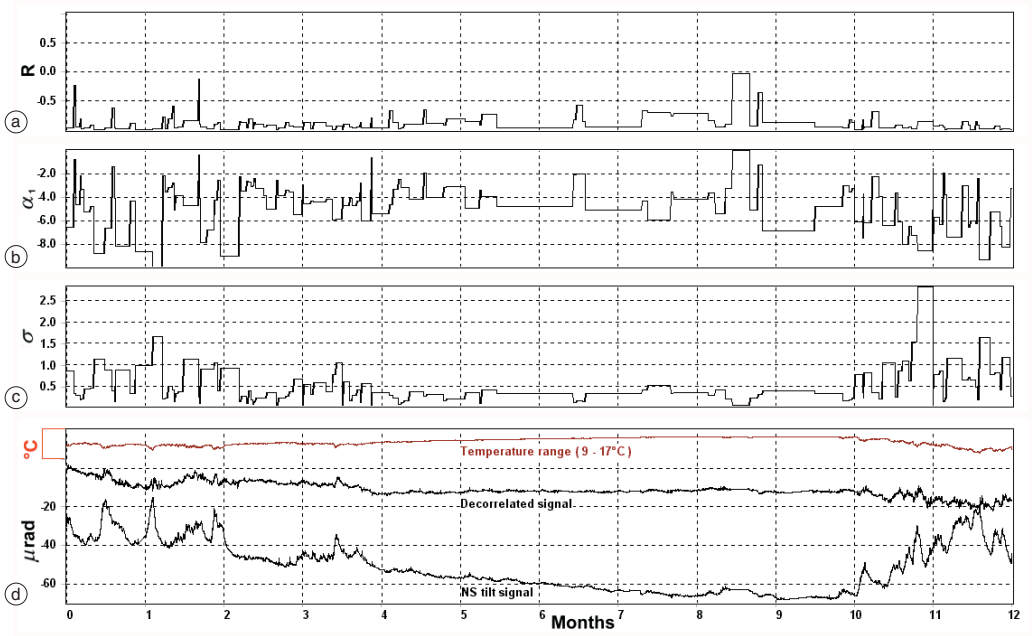

Fig. 14a-d. The thermal correction is applied to the NS tilt component recorded by DMB in 2001. The decorrelated signal undergoes a contraction in comparison to the original signal showing an inclination towards S (subsidence).

computed and indicated a good global fit of the data (fig. 14a-c).

In both uplift and subsidence, the statistical decorrelation provided good results, in accordance with the other geodetic data (from levelling and GPS).

15. Conclusions

The correct estimate of the variations of ground inclination induced by volcanic activity implies a knowledge of the many causes that influence the tilt signal recorded, such as environmental temperature, atmospheric pressure, rainfall, oscillation of the water table, pressure and ocean loading, earth tides, ground coupling, etc. For this reason, tilt data must be compared with those acquired by the other geodetic methods such as levellings, GPS and SAR and, in the case in which the stations are near to the sea, it is also necessary to consider the tide-gauge data.

Almost 15 years of data acquired in different sites have yielded useful information on ground deformation, and the data have disclosed two uplifts of modest entity, but that give the idea that a net of this type shows traces of the inversions of ground displacement.

Besides we have tried a quantitative approach to estimate the thermal effect, applying a statistical method to data recorded in recent years; in this analysis we reported only the results related to the most meaningful component (NS) of the most sensitive station (DMB) in two years, 2000 and 2001, in which the deformation shows very different trends.

This test also shows both the reliability of the data and the correctness of the procedure used that also allows us to assign the error committed on the fit. In addition, we are proceeding to a whole renovation of the tilt network and beginning to install borehole sensors and improve the methods of correction of the signals to make them applicable to all data recorded to date.

REFERENCES

ACHILLI, V., O. AL-BAYARI, I. AQUINO, P. BERARDINO, S. BORGSTROM, G. CECERE, C. DEL GAUDIO, P. DE MARTINO, M. FABRIS, D. GALLUZZO, R. LANARI, W. MARZOCCHI, A. MENIN, G.P. RICCIARDI, C. RICCO, G. SALEMI, E. SANSOSTI, V. SEPE, V. SINISCALCHI and M. TESAURO (2001): Un approccio multimetodologico per il monitoraggio geodetico dell'area flegrea, in *Atti del I Convegno AUTEC, Napoli 17-18 Maggio 2001*, 159-168.

AGI (Applied Geomechanics Incorporated) (1995): Tiltmeter temperature coefficients: source, definition and use to improve accuracy, *Report n. B-95-1005, Rev. C*.

AGI (Applied Geomechanics Incorporated) (1997): 700 series platform and surface mount tiltmeters, *Manual n. B-88-1016*.

AGI (Applied Geomechanics Incorporated) (1998): Computation of cross-axis tilts for biaxial clinometers and tiltmeters, *Report n. A-98-1003*.

ASTE, J.P., P.A. BLUM, J.L. BORDES, B. MEMIER and B. SALEH (1986): Utilisation d'un clinometre à trés haute resolution pour l'etude du comportement des ouvrages de génie civil, *Rev. Fr. Geotech.*, **34**, 57-67.

BERGER, J. (1975): A note on thermoelastic strains and tilts, *J. Geophys. Res.*, **80**, 274-277.

BONACCORSO, A. and S. GAMBINO (1997): Impulsive tilt variations on Mount Etna Volcano (1990-1993), *Tectonophysics*, **270**, 115-125.

BRAITENBERG, C. (1999): Estimating the hydrologic induced signal in geodetic measurements with predicitive filtering methods, *Geophys. Res. Lett.*, **26**, 775-778.

BRAITENBERG, C., I. NAGY, M. NEGUSINI, C. ROMAGNOLI, M. ZADRO and S. ZERBINI (2001): Geodetic measurements at the northern border of the Adria plate, *J. Geodyn.*, **32** (Millennium Issue), 267-286.

BRIOLE, P. (1987): *Les Reseaux d'Inclinometrie de l'Etna et de Pozzuoli*, IPG Paris.

DADISP (Data Analysis and Display Software) (1996): *Function Reference Manual*, DSP Development Corporation.

DAL MORO, G. and M. ZADRO (1998): Subsurface deformations induced by rainfall and atmospheric pressure: tilt/strain measurements in the NE-Italy seismic area, *Earth Planet. Sci. Lett.*, **164**, 193-203.

DAVIS, P.M., P.A. RYDELEK, D.C. AGNEW and A.T. OKAMURA (1987): Observation of tidal tilt on Kilauea Volcano, Hawaii, *Geophys. J. R. Astron. Soc.*, **90**, 233-244.

DAVIS, J.C. (2002): *Statistics and Data Analysis in Geology* (John Wiley & Sons), pp. 638.

DZURISIN, D. (1992): Electronic tiltmeters for volcano monitoring: lessons from Mount St. Helens, *U.S. Geol. Surv. Bull.*, 69-83.

HARRISON, J.C. (1976): Cavity and topographic effects in tilt and strain measurements, *J. Geophys. Res.*, **81**, 319-328.

HARRISON, J.C. and K. HERBST (1977): Thermoelastic strains and tilts revised, *Geophys. Res. Lett.*, **4**, 535-537.

IMBÒ, G. (1939): Oscillazioni dell'edificio vulcanico concomitanti le recrudescenze eruttive del vulcano, *Rend. R. Accad. Naz. Lincei*, **XXIX**.

IMBÒ, G. (1959): Oscillazioni a periodo semidiurno lunare nell'attività eruttiva vesuviana, in *Atti dell'8° Convegno AGI.*

JENTZSCH, G., M. LIEBING and A. WEISE (1993): Deep boreholes for high resolution tilt recordings, *Bull. Inf. Marees Terrestres*, **115**, 8498-8506.

JENTZSCH, G., S. GRAUPNER, A. WEISE, H. ISHII and S. NAKAO (2002): Environmental effects in tilt data of Nokogiriyama Observatory, *Bull. Inf. Marees Terrestres*, **137**, 10931-10936 (extended abstract).

KÜMPEL, H.J. (1983): The effect of variations on the groundwater table on borehole tiltmeters, in *Proceedings of the 9th International Symposium on Earth Tides*, edited by J.T. KUO (New York), 33-45.

KÜMPEL, H.J. (1986): Model calculations for rainfall induced tilt and strain anomalies, in *Proceedings of the 10th International Symposium on Earth Tides*, edited by R. VIEIRA (Madrid), 889-903.

LO BASCIO, A. and M.T. QUAGLIARIELLO (1968): Risultati ottenuti dallo studio della deviazione apparente della verticale alla stazione di Napoli, in *Atti del 17° Convegno AGI*, 440-457.

LUONGO, G., C. DEL GAUDIO, F. OBRIZZO and C. RICCO (1998): La rete tiltmetrica OV-IPG operante ai Campi Flegrei, in *Atti del 74° Congresso Nazionale della Società Geologica Italiana*, A.

MANZONI, G. (1972): Misure clinometriche, *Quad. Ric. Sci.*, **83**, 198-208.

MELCHIOR, P. (1978): *The Tides of the Planet Earth* (Pergamon Press, Oxford), pp. 609.

OPPENHEIM, A.V. and R.W. SCHAFER (1975): *Digital Signal Processing* (Prentice-Hall).

ORSI, G., L. CIVETTA, C. DEL GAUDIO, S. DE VITA, M.A. DI VITO, R. ISAIA, S.M. PETRAZZUOLI, G.P. RICCIARDI and C. RICCO (1999): Short-term ground deformations and seismicity in the resurgent Campi Flegrei caldera (Italy): an example of active block-resurgence in a densely populated area, *J. Volcanol. Geotherm. Res.*, **91**, 415-451.

PERSICO, E. (1962): *Introduzione alla Fisica Matematica* (Zanichelli), 309-328.

RICCO, C., C. DEL GAUDIO, F. OBRIZZO and G. LUONGO (1991): Misurazioni delle variazioni delle inclinazioni del suolo ai Campi Flegrei, in *Atti del 10° Convegno annuale GNGTS*, 1003-1012.

RICCO, C., C. DEL GAUDIO, F. OBRIZZO and G. LUONGO (1994): Monitoraggio dei movimenti lenti del suolo in aree di vulcanismo attivo: Campi Flegrei, *Boll. Soc. It. Fotogramm. Topogr.*, **3**, 33-68.

RICCO, C., C. DEL GAUDIO, F. QUARENI and W. MARZOCCHI (2000): Spectral analysis of the clinometric data at the Phlegraean Fields from 1992 to 1998, *Ann. Geofis.*, **43** (5), 939-950.

ROSI, M., L. VEZZOLI, P. ALEOTTI and M. DE CENSI (1995): Interaction between caldera collapse and eruptive dynamics during the Campanian Ignimbrite eruption, Phlegraean Fields, Italy, *Bull. Volcanol.*, **57**, 541-554.

SCANDONE, R. and L. GIACOMELLI (1998): *Vulcanologia. Principi Fisici e Metodi d'Indagine* (Liguori Editore, Napoli), pp. 608.

SLEEMAN, R., H.W. HAAK, M.S. BOS and J.J.A. VAN GEND (2000): Tidal tilt observations in the Netherlands using shallow borehole tiltmeters, *Phys. Chem. Earth A*, **25** (4), 415-420.

WEISE, A., G. JENTZSCH, A. KIVINIEMI and J. KÄÄRIÄINEN (1999): Comparison of long-period tilt measurements: results from the two clinometric stations Metsähovi and Lohja, Finland, *J. Geodyn.*, **27**, 237-257.

WOLFE, J.E., E. BERG and G.H. SUTTON (1981): The change in strain comes mainly from the rain: Kipapa, Oahu, *Bull. Seismol. Soc. Am.*, **71**, 1625-635.

ZADRO, M. and C. BRAITENBERG (1999): Measurements and interpretations of tilt-strain gauges in seismically active areas, *Earth Sci. Rev.*, **47**, 151-187.

(received June 5, 2003;
accepted December 19, 2003)